Carbohydrate Research 440-441 (2017) 51–62

Contents lists available at ScienceDirect

Carbohydrate Research

journal homepage: www.elsevier.com/locate/carres

Structural analysis of rebaudioside A derivatives obtained by *Lactobacillus reuteri* 180 glucansucrase-catalyzed trans-α-glucosylation

Gerrit J. Gerwig [a, b, 1], Evelien M. te Poele [a, 1], Lubbert Dijkhuizen [a, *], Johannis P. Kamerling [a, b]

[a] Microbial Physiology, Groningen Biomolecular Sciences and Biotechnology Institute (GBB), University of Groningen, Nijenborgh 7, 9747 AG, Groningen, The Netherlands

[b] NMR Spectroscopy, Bijvoet Center for Biomolecular Research, Utrecht University, Padualaan 8, 3584 CH, Utrecht, The Netherlands

ARTICLE INFO

Article history:
Received 17 November 2016
Received in revised form
18 January 2017
Accepted 19 January 2017
Available online 31 January 2017

Keywords:
Stevia rebaudiana
Sweetener
Steviol glycosides
Carbohydrate
NMR spectroscopy
Glycobiotechnology

ABSTRACT

The wild-type Gtf180-ΔN glucansucrase enzyme from *Lactobacillus reuteri* 180 was found to catalyze the α-glucosylation of the steviol glycoside rebaudioside A, using sucrose as glucosyl donor in a trans-glucosylation process. Structural analysis of the formed products by MALDI-TOF mass spectrometry, methylation analysis and NMR spectroscopy showed that rebaudioside A is specifically α-D-glucosylated at the steviol C-19 β-D-glucosyl moiety (55% conversion). The main product is a mono-(α1 → 6)-glucosylated derivative (RebA-G1). A series of minor products, up to the incorporation of eight glucose residues, comprise elongations of RebA-G1 with mainly alternating (α1 → 3)- and (α1 → 6)-linked glucopyranose residues. These studies were carried out in the context of a program directed to the improvement of the taste of steviol glycosides via enzymatic modification of their naturally occurring carbohydrate moieties.

1. Introduction

The leaves of the *Stevia rebaudiana* BERTONI plant contain a high variety of sweet substances, called steviol glycosides [1,2], and so far more than 40 different structures have been elucidated (see review Ref. [3]). Stevioside (~5–20% w/w of dried leaves) and rebaudioside A (~2–5% w/w of dried leaves) are the most abundant components (Fig. 1), tasting about 200–300 times sweeter than sucrose (0.4% aqueous solution). Structurally, steviol glycosides have *ent*-13-hydroxykaur-16-en-19-oic acid as aglycone, called steviol, but are differing in carbohydrate composition at the C-13-*tert*-hydroxyl and C-19-carboxyl functions.

Due to the growing awareness and concerns for human health related to excessive consumption of sugar (sucrose), the application of steviol glycosides as non-caloric bio-alternatives for sucrose and as substitutes for artificial (synthetic) sweeteners is strongly promoted nowadays [4–8]. Since a couple of years, steviol glycosides have been permitted for use as food additive and sweetener in the USA [9] and in Europe (E960) [10,11]. However, despite their intense sweetness and diverse beneficial pharmacological properties [12–15], the main drawback for successful commercialization of *Stevia* sweeteners is their slight bitterness and unpleasant (metallic) aftertaste, experienced by more than half of the human population.

For natural steviol glycosides with β-D-glucopyranosyl units as constituents, it has been reported that the ratio of the number of glucose units at the C-13 site to that at the C-19 site of the steviol core has a relationship with the sweetness as well as with the quality of taste of the steviol glycosides [16,17]. To improve the

Abbreviations: FID, free induction decay; FWHM, full width at half maximum; GLC-EI-MS, gas-liquid chromatography electron impact mass spectrometry; HPAEC, high-pH anion-exchange chromatography; HSQC, ^{1}H-detected hetero-nuclear single-quantum coherence spectroscopy; MALDI-TOF-MS, matrix-assisted laser desorption ionization time-of-flight mass spectrometry; MLEV, composite pulse devised by M. Levitt; NMR, nuclear magnetic resonance; RebA, rebaudioside A; RebB, rebaudioside B; ROESY, rotating-frame nuclear Overhauser enhancement spectroscopy; Ste, stevioside; TLC, thin-layer chromatography; TOCSY, total correlation spectroscopy; UV–VIS, ultraviolet–visible; WEFT, water eliminated Fourier transform.

* Corresponding author.
E-mail address: L.Dijkhuizen@rug.nl (L. Dijkhuizen).

[1] These authors contributed equally to this work.

http://dx.doi.org/10.1016/j.carres.2017.01.008

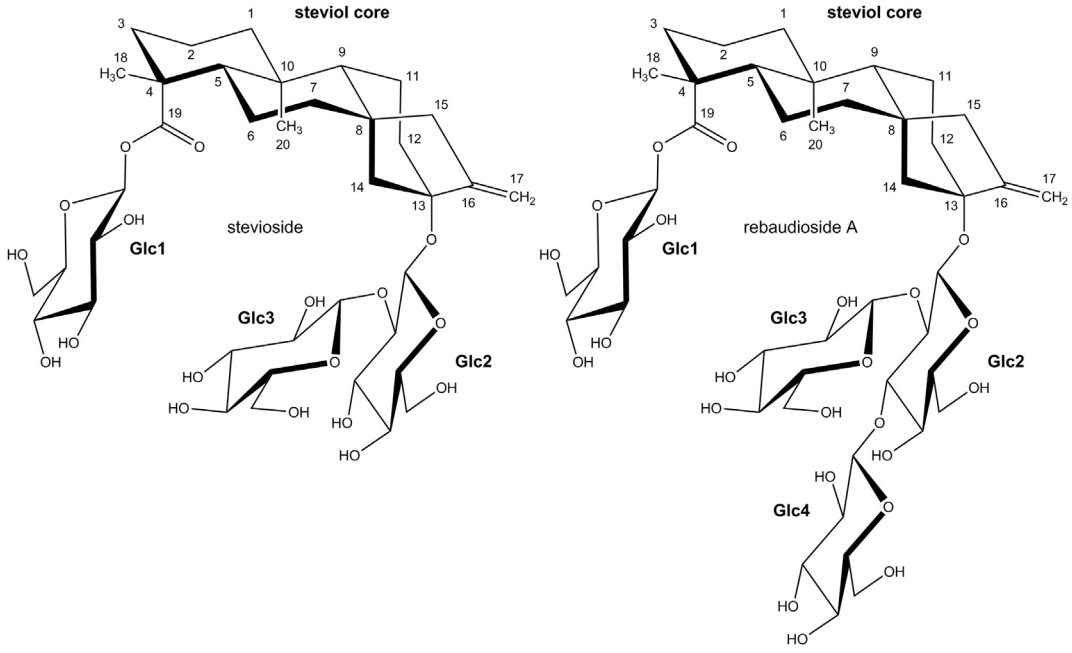

Fig. 1. Structures of stevioside (Ste) and rebaudioside A (RebA), occurring as main components in the leaves of the *Stevia rebaudiana* plant.

taste, especially for food applications, chemical and enzymatic modifications of the carbohydrate moieties of specific steviol glycosides have been investigated, and showed promising results [3,16,18–25].

Glucansucrase enzymes from probiotic lactic acid bacteria, when incubated with sucrose as donor/acceptor substrate, produce (sucrose-linked) α-D-glucans with different linkage types depending on the specific strain/specific glucansucrase used [26]. In the presence of sucrose plus non-sucrose acceptor substrates, these enzymes additionally catalyze the formation of oligosaccharide/glycoconjugate products [27]. Previously, it has been shown that the glucansucrase enzyme Gtf180 from *Lactobacillus reuteri* 180 and its recombinant truncated Gtf180-ΔN derivative were able to synthesize from sucrose an α-D-glucan (EPS180) with ~69% (α1 → 6) and ~31% (α1 → 3) linkages, the latter being present both in the main chain, although not in a successive way, and as branching points (Fig. 2) [28]. More recently, it has been shown that EPS180 also contains low amounts (<1%) of (α1 → 4) linkages [29], whereas incubations with mutant Gtf180-ΔN enzymes led to bioengineered (1 → 3,1 → 4,1 → 6)-α-D-glucans with up to 12% (α1 → 4) linkages [29–31]. For the latter polysaccharides, Glc(α1 → 4) and Glc(α1 → 4)Glc(α1 → 4) units were found to occur in terminal positions.

With a focus on enzymatic modifications of steviol glycosides to produce derivatives with improved organoleptic properties, we have incubated rebaudioside A with sucrose and the wild-type Gtf180-ΔN glucansucrase enzyme from *Lb. reuteri* 180. Here, we present detailed structural analyses by MALDI-TOF mass spectrometry, methylation analysis and 1D/2D $^{1}H/^{13}C$ NMR spectroscopy of obtained α-D-glucopyranosylated products.

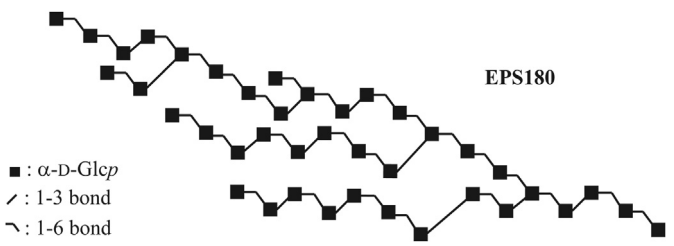

Fig. 2. Composite structure of the extracellular polysaccharide EPS180 from the lactic acid bacterium *Lactobacillus reuteri* 180 [28].

2. Results and discussion

2.1. Incubation of rebaudioside A with the Gtf180-ΔN glucansucrase enzyme and sucrose

Inspection of the molecular structure of rebaudioside A {RebA, 13-[(2-*O*-β-D-glucopyranosyl-3-*O*-β-D-glucopyranosyl-β-D-glucopyranosyl)oxy]*ent*-kaur-16-en-19-oic acid β-D-glucopyranosyl ester} (Fig. 1) shows four Glc residues (**Glc1**, **Glc2**, **Glc3** and **Glc4**) with a total of fourteen free hydroxyl groups, which can act as acceptors for transglucosylation reactions. In view of the reported enzymatic activity of the wild-type Gtf180-ΔN glucansucrase enzyme from *Lb. reuteri* 180 (Section 1) [28–31], at first instance, elongations at HO-3, HO-4 and HO-6 are expected.

RebA (50 mM) was incubated at 37 °C with 10 U/mL wild-type Gtf180-ΔN enzyme in sodium acetate buffer, pH 4.7, containing 1.0 M sucrose. After 3 h, a second batch of 1.0 M sucrose was added to the reaction mixture, and the incubation was prolonged for 21 h. After removal of glucose, fructose, gluco-oligo/polysaccharide (products of the "natural activity" of the enzyme), protein material, and residual sucrose from the reaction mixture via solid-phase extraction, HPLC analysis of the (α-glucosylated) RebA mixture showed a complex pattern of peaks, as visualized in Fig. 3. Fraction **F1** had the same retention time as the acceptor substrate RebA. For further analysis, fractions **F1**-**F9** were isolated.

MALDI-TOF-MS analysis of the fractions **F1**-**F9** showed a series of quasi-molecular ions $[M+Na]^{+}$, in accordance with an extension of RebA (**F1**) with one (**F2**) to eight (**F9**) glucose residues, respectively (Supplementary Information Fig. S1). However, in view of the HPLC peak clusters within some fractions, groups of isomeric components with the same molecular mass can be expected. Integration of the HPLC peaks in Fig. 3 revealed that 55% of RebA

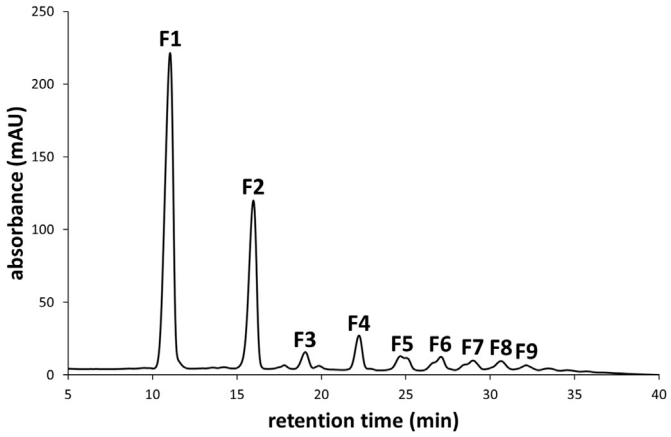

Fig. 3. HPLC profile after a 24-h incubation of RebA (50 mM) with wild-type Gtf180-ΔN enzyme (10 U/mL) and sucrose (1.0 M was added at t = 0 and 3 h) at pH 4.7 and 37 °C.

was converted into glucosylated products [mainly **F2** (25%) and minor amounts of **F3** to **F9** (in total 30%)]. To obtain detailed structural information about the generated RebA derivatives, fractions **F1**-**F9** were subjected to methylation analysis and NMR spectroscopy.

As literature NMR data of RebA were mostly available for solvent systems differing from D_2O [e.g. C_5D_5N, C_5D_5N+$(CD_3)_2SO$, $(CD_3)_2SO$, CD_3OD, CD_3OD+D_2O] [32–39], and in the present study the acceptor substrate and the enzymatic products were measured in D_2O, a full 1D/2D $^1H/^{13}C$ NMR analysis of commercial RebA in D_2O at 334 K was carried out. The results of these analyses are summarized in the Supplementary Information (report and Figs. S2–S5). ^1H and ^{13}C chemical shifts of RebA are shown in Tables 1 and 2. For an explanation of the code system used, see Fig. 4.

2.2. Structural analysis of HPLC fraction *F1*

NMR analysis of fraction **F1** confirmed the presence of acceptor substrate RebA (Fig. 5, ^1H NMR spectrum of **F1**, identical to Supplementary Information Fig. S3; Tables 1 and 2). Methylation analysis (Table 3) revealed the presence of terminal Glc*p* and 2,3-di-O-substituted Glc*p* in the molar ratio of 3:1, as expected for RebA.

2.3. Structural analysis of HPLC fraction *F2*

Methylation analysis of **F2** (RebA+1Glc) (Table 3) showed a 3:1 molar ratio for terminal Glc*p* and 2,3-di-O-substituted Glc*p*, indicating that the additional Glc*p* residue is attached to a terminal Glc*p* residue of RebA. The detection of a 6-mono-O-substituted Glc*p* residue suggested a product with a Glc*p*(1 → 6) extension.

The ^1H NMR spectrum of **F2** (Fig. 5; enlarged anomeric region in Supplementary Information Fig. S6) exhibited the typical steviol core signal pattern as seen for RebA (**F1**). Besides the four β-anomeric ^1H signals related to RebA (**Glc1**, δ_H 5.410; **Glc2**, δ_H 4.700; **Glc3**, δ_H 4.801; **Glc4**, δ_H 4.699), one α-anomeric ^1H resonance (δ_H 4.865; $J_{1,2}$ 3.7 Hz), partly overlapping with one steviol C-17 proton, was observed, stemming from a new α-linked Glc residue (**Glc5**). The latter signal correlated with a ^{13}C resonance at δ_C 99.5 in the HSQC spectrum (Fig. 6).

In a similar way as described for RebA in the Supplementary Information, using 2D NMR spectroscopy (TOCSY with different mixing times, ROESY and HSQC, Fig. 6), the $^1H/^{13}C$ chemical shifts of the steviol core (Table 1) and the five Glc residues (Table 2) of **F2** were assigned. The ^1H and ^{13}C chemical shift sets of **Glc2**, **Glc3** and **Glc4** are nearly identical to those of **F1** (RebA), suggesting that no modifications had occurred in the carbohydrate moiety at the

Table 1
^1H and ^{13}C chemical shifts (δ)[a] for the steviol part of RebA (fraction **F1**), α-glucosylated RebA products [fractions **F2** (RebA+1Glc), **F3**P1 (RebA+2Glc), **F3**P2 (RebA+2Glc) and **F4** (RebA+3Glc)], alkaline-treated fractions **F1** to **F4** = RebB (fraction **F1-4S**) and **Ste** (stevioside), recorded in D_2O at 334 K. For structures, see Fig. 4.

Carbon[b]	**F1**		**F2**		**F3**P1		**F3**P2		**F4**		**F1-4S**		**Ste**		**RebA** (C_5D_5N)[c]	
Number	^1H	^{13}C	^1H	^{13}C	^1H	^{13}C	^1H	^{13}C	^1H	^{13}C	^1H	^{13}C	^1H	^{13}C	^1H	^{13}C
1	0.81	41.6	0.81	41.6	0.82	41.5	0.81	41.6	0.82	41.5	0.78	41.8	0.82	41.3	0.78	41.2
	1.81		1.82		1.80		1.81		1.82		1.78		1.82		1.77	
2	1.40	20.3	1.30	20.3	1.30	20.3	1.30	20.3	1.30	20.4	1.25	20.4	1.31	20.5	1.45	19.9
	1.75		1.60		1.51		1.52		1.51		1.37		1.60		2.22	
3	1.07	38.8	1.04	38.9	1.06	38.9	1.06	38.9	1.06	38.9	0.88	40.0	1.06	38.6	1.03	37.3
	2.07		2.06		2.04		2.04		2.04		1.96		2.05		2.35	
5	1.15	58.1	1.11	58.1	1.14	58.1	1.14	58.1	1.15	58.0	0.94	57.9	1.14	57.9	1.05	57.8
6	1.60	22.8	1.68	22.8	1.82	22.9	1.82	22.9	1.84	22.9	1.85	23.0	1.65	22.8	1.92	22.6
	1.80		1.80		2.04		2.04		2.04		2.03		1.82		2.46	
7	1.41	42.5	1.39	42.5	1.40	42.4	1.41	42.5	1.41	42.5	1.37	42.3	1.41	42.2	1.30	42.2
	1.50		1.51		1.49		1.49		1.50		1.47		1.47		1.30	
9	0.98	54.7	0.97	54.8	0.97	54.8	0.97	54.8	0.97	54.7	0.95	55.0	0.96	54.6	0.88	54.5
11	1.70	23.1	1.70	22.9	1.66	22.9	1.66	22.9	1.68	23.0	1.67	22.5	1.78	22.9	1.68	21.1
	1.82		1.83		1.80		1.81		1.80		1.80		1.83		1.68	
12	1.49	38.2	1.47	38.1	1.48	38.2	1.48	38.2	1.48	38.1	1.48	39.1	1.47	37.7	2.00	37.3
	1.90		1.89		1.88		1.88		1.88		1.88		1.89		2.25	
14	1.42	45.7	1.41	45.6	1.41	45.8	1.41	45.8	1.40	45.8	1.42	46.1	1.40	45.8	1.81	45.0
	2.12		2.10		2.10		2.10		2.12		2.15		2.14		2.66	
15	2.07	48.5	2.03	48.5	2.05	48.6	2.05	48.5	2.05	48.5	2.05	48.8	2.05	48.4	2.05	48.2
	2.12		2.12		2.10		2.11		2.09		2.08		2.09		2.05	
17	4.875	105.7	4.870	105.8	4.875	105.6	4.875	105.7	4.875	105.7	4.875	105.7	4.872	105.4	5.01	105.1
	5.065		5.060		5.040		5.040		5.038		5.044		5.035		5.64	
18	1.175	29.6	1.174	29.5	1.175	29.5	1.175	29.6	1.174	29.4	1.013	30.0	1.175	29.3	1.25	28.8
20	0.827	16.8	0.830	16.8	0.827	16.9	0.830	16.9	0.822	16.9	0.881	16.9	0.827	16.7	1.32	16.0

[a] In ppm relative to internal acetone (δ 2.225 for ^1H and δ 31.07 for ^{13}C).
[b] As ^{13}C data have been deduced from HSQC measurements, ^{13}C chemical shifts in D_2O are missing for C-4, C-8, C-10, C-13, C-16 and C-19.
[c] For comparison, NMR data of RebA recorded in C_5D_5N at 271 K (99.96 atom% D; solvent calibration: δ 8.74 for ^1H and δ 150.3 for ^{13}C) are included [35].

Table 2
^{1}H and ^{13}C chemical shifts (δ)[a] for the Glc*p* residues of RebA (fraction **F1**), α-glucosylated RebA products [fractions **F2** (RebA+1Glc), **F3**P1 (RebA+2Glc), **F3**P2 (RebA+2Glc) and **F4** (RebA+3Glc)], alkaline-treated fractions **F1** to **F4** = RebB (fraction **F1-4S**) and **Ste** (stevioside), recorded in D_2O at 334 K. For structures, see Fig. 4.

Residue	**F1**		**F2**		**F3**P1		**F3**P2[b]		**F4**		**F1-4S**		**Ste**	
	^{1}H	^{13}C	^{1}H	^{13}C	^{1}H	^{13}C	^{1}H	^{13}C	^{1}H	^{13}C	^{1}H	^{13}C	^{1}H	^{13}C
Glc1(β1→C-19)														
H-1	5.400	95.6	5.410	95.6	5.426	95.7	5.425	95.7	5.425	95.8	–	–	5.400	95.6
H-2	3.43	73.7	3.44	73.6	3.44	74.0	3.44	73.6	3.45	73.8	–	–	3.45	73.6
H-3	3.50	78.0	3.49	77.9	3.50	77.6	3.51	77.8	3.51	78.0	–	–	3.50	78.0
H-4	3.40	71.0	3.47	71.0	3.45	70.5	3.45	70.4	3.45	70.6	–	–	3.39	71.0
H-5	3.50	78.0	3.67	77.0	3.71	77.3	3.69	77.0	3.69	77.0	–	–	3.50	77.5
H-6a	3.82	62.2	3.87	*67.0*[c]	3.89	*67.5*	3.91	*67.0*	3.89	*67.0*	–	–	3.82	62.3
H-6b	3.67		3.69		3.70		3.69		3.70		–		3.67	
Glc2(β1→C-13)														
H-1	4.704	97.6	4.700	97.5	4.720	97.6	4.715	97.6	4.700	97.6	4.704	97.8	4.707	97.4
H-2	3.68	*80.3*	3.67	*80.5*	3.67	*80.5*	3.68	*80.4*	3.67	*80.5*	3.68	*80.4*	3.50	*82.3*
H-3	3.81	*86.8*	3.81	*87.0*	3.82	*86.7*	3.82	*86.7*	3.81	*87.0*	3.82	*87.0*	3.62	77.8
H-4	3.46	70.3	3.46	70.5	3.45	70.5	3.46	70.5	3.46	70.6	3.45	70.5	3.35	71.4
H-5	3.44	77.5	3.44	77.5	3.42	77.5	3.43	77.5	3.45	77.5	3.40	78.0	3.33	77.4
H-6a	3.83	62.5	3.84	62.5	3.82	62.7	3.84	62.5	3.85	62.4	3.81	62.8	3.80	62.4
H-6b	3.67		3.67		3.67		3.67		3.67		3.66		3.65	
Glc3(β1→2)														
H-1	4.800	103.6	4.801	103.5	4.810	103.5	4.810	103.6	4.802	103.6	4.817	103.7	4.672	104.6
H-2	3.21	76.0	3.21	75.9	3.22	76.0	3.23	75.8	3.22	75.9	3.24	76.2	3.27	75.9
H-3	3.41	77.5	3.41	77.5	3.41	77.5	3.41	77.5	3.40	77.4	3.39	78.0	3.45	77.3
H-4	3.25	71.9	3.25	72.0	3.24	71.9	3.25	71.8	3.24	72.0	3.27	72.2	3.30	71.5
H-5	3.33	77.5	3.33	77.5	3.33	77.2	3.34	77.5	3.32	77.6	3.34	77.8	3.34	77.4
H-6a	3.81	63.0	3.81	63.0	3.81	63.0	3.81	62.6	3.81	63.0	3.82	63.3	3.82	62.5
H-6b	3.61		3.61		3.62		3.61		3.62		3.62		3.65	
Glc4(β1→3)														
H-1	4.697	103.8	4.699	103.8	4.700	103.8	4.702	103.9	4.700	103.7	4.714	104.2		
H-2	3.32	75.0	3.31	75.0	3.32	75.0	3.32	74.9	3.31	75.0	3.32	75.4		
H-3	3.45	77.5	3.45	77.6	3.45	77.5	3.46	77.6	3.45	77.5	3.45	77.8		
H-4	3.35	71.0	3.35	71.0	3.35	71.0	3.37	71.0	3.35	71.4	3.37	71.7		
H-5	3.33	77.5	3.33	77.5	3.33	77.5	3.34	77.5	3.33	77.4	3.35	77.5		
H-6a	3.85	63.0	3.85	62.8	3.85	62.7	3.84	62.7	3.83	62.5	3.85	62.6		
H-6b	3.65		3.66		3.65		3.66		3.65		3.66			
Glc5			(α1→6)		(α1→6)		(α1→6)		(α1→6)					
H-1			4.865	99.5	4.875	99.5	4.873	99.5	4.875	99.2				
H-2			3.47	73.1	3.49	71.0	3.55	71.6	3.57	72.0				
H-3			3.65	74.9	3.66	73.7	3.79	*81.5*	3.77	*82.3*				
H-4			3.35	71.0	3.42	70.1	3.59	71.6	3.60	73.0				
H-5			3.63	73.2	3.80	71.8	3.65	73.5	3.65	73.3				
H-6a			3.75	62.0	3.88	*67.5*	3.83	62.5	3.84	62.5				
H-6b			3.65		3.65		3.66		3.66					
Glc6′/Glc6					(α1→6)		(α1→3)		(α1→3)					
H-1					4.875	99.5	5.275	100.0	5.259	101.2				
H-2					3.48	73.4	3.50	73.2	3.52	73.5				
H-3					3.65	74.7	3.68	75.0	3.67	75.0				
H-4					3.36	71.2	3.38	72.0	3.48	71.5				
H-5					3.64	73.5	3.93	73.4	4.09	72.2				
H-6a					3.79	62.5	3.76	62.4	3.94	*67.0*				
H-6b					3.65		3.66		3.64					
Glc7									(α1→6)					
H-1									4.875	99.3				
H-2									3.47	73.1				
H-3									3.65	74.5				
H-4									3.34	71.3				
H-5									3.64	73.2				
H-6a									3.75	62.5				
H-6b									3.67					

[a] In ppm relative to the signal of internal acetone (δ 2.225 for ^{1}H and δ 31.07 for ^{13}C).
[b] For **F3**P2 the δ values of the major component RebA-G2b are given. The δ values of the anomeric protons of the carbohydrate moiety at the steviol C-19 site of the minor component RebA-G2c are: **Glc1** H-1, δ_H 5.410; **Glc5** H-1, δ_H 4.857; **Glc6** H-1, δ_H 5.265.
[c] Substituted carbon positions are indicated in italics.

steviol C-13 site. The TOCSY **Glc5** H-1 track (δ_H 4.865) showed the complete scalar coupling network H-1,2,3,4,5,6a,6b, and combined with the **Glc5** C-1–C-6 set of chemical shifts, a terminal Glc(α1 → 6) unit is indicated. Based on the inter-residual ROESY cross-peaks between **Glc5** H-1 (δ_H 4.865) and **Glc1** H-6a/b (δ_H 3.87/3.69) (Fig. 6), combined with the ^{13}C downfield shift of ~5 ppm for **Glc1** C-6 (δ_C 67.0; RebA **Glc1** C-6: δ_C 62.2) (HSQC spectrum, Fig. 6), a **Glc5**(α1 → 6)**Glc1** disaccharide element could be established. Note that **Glc5** H-1 of the steviol core ester-bound β-isomaltose in **F2** (δ_H 4.865, T = 334 K) resonates clearly upfield from the anomeric proton of the terminal Glc(α1 → 6) residue in free β-isomaltose (δ_H ~4.96; T = 300 K) [40]. The absence of → 3)Glc*p*(1 → or → 4)Glc*p*(1 → elements in the methylation analysis of **F2** (Table 3) together with the absence of an α-anomeric ^{1}H signal at δ_H ~5.27,

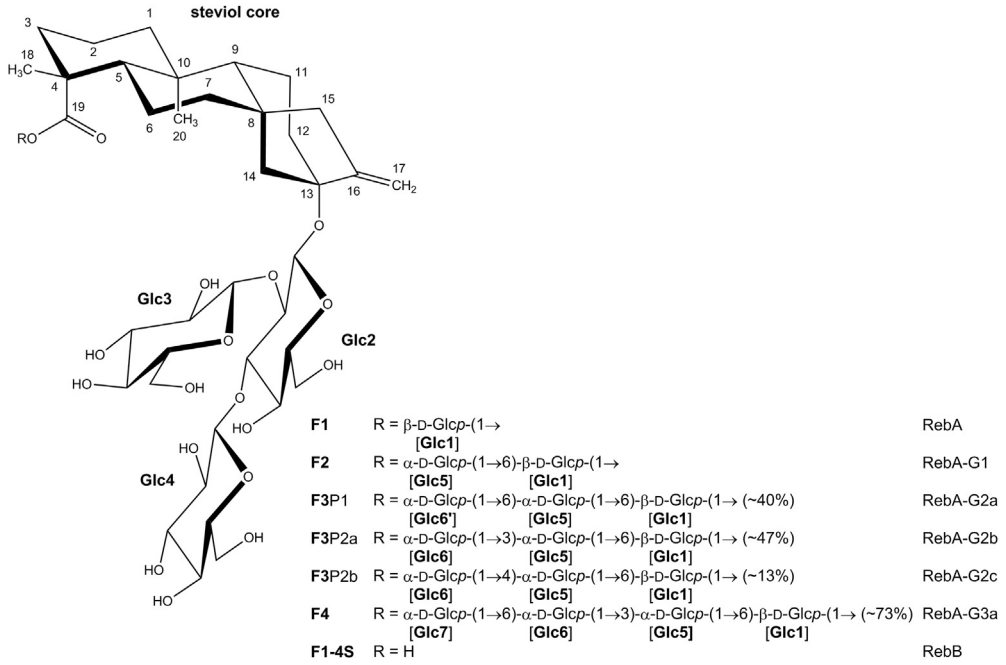

Fig. 4. Structures of RebA (**F1**), α-glucosylated RebA products [fractions **F2** (RebA+1Glc), **F3**P1 (RebA+2Glc), **F3**P2a (RebA+2Glc), **F3**P2b (RebA+2Glc) and **F4** (RebA+3Glc)] and alkaline-treated fractions **F1**-**F4** = RebB (fraction **F1-4S**). [**Glc1**], etc. are denotations for the glucose residues attached at the steviol C-19 site.

typical for a terminal Glc(α1 → 3) or Glc(α1 → 4) residue (see fraction **F3**P2, Section 2.4), supports the absence of such extensions at **Glc1**.

To confirm the exclusive introduction of the Glc residue (**Glc5**) at the steviol C-19 glucosyl moiety (**Glc1**) of RebA, and not at the steviol C-13 trisaccharide part, fraction **F2** was subjected to alkaline conditions (1.0 M NaOH, 2.5 h, 80 °C), which should specifically cleave the C-19 carboxyl-glucosyl ester linkage, leaving the glycosylation of the steviol C-13 part intact. To check the reaction conditions, the alkaline-induced transition of RebA (**F1**) into rebaudioside B (RebB; Fig. 4; Tables 1 and 2) was carried out as a positive control. The formed product from **F2** (denoted as **F1-4S**), isolated via reversed phase column chromatography, was investigated by MALDI-TOF-MS ($[M+Na]^+$, *m/z* 827.3), methylation analysis (terminal Glc*p*: 2,3-di-O-substituted Glc*p* = 2:1) and NMR spectroscopy (1D, TOCSY, HSQC, ROESY; presence of **Glc2**, **Glc3** and **Glc4**, absence of **Glc1** and **Glc5**; Tables 1 and 2), and shown to be identical with reference RebB. The 1D ^{1}H NMR and HSQC spectra of **F1-4S** (RebB) are presented in Supplementary Information Fig. S7.

In summary, the mono-transglucosylated product from fraction **F2** is RebA with a Glc(α1 → 6) extension at **Glc1** attached to the steviol C-19 site. It is chemically formulated as 13-[(2-*O*-β-D-glucopyranosyl-3-*O*-β-D-glucopyranosyl-β-D-glucopyranosyl)oxy]*ent*-kaur-16-en-19-oic acid 6-*O*-α-D-glucopyranosyl-β-D-glucopyranosyl ester, and will be called RebA-G1 (Fig. 4).

Interestingly, the β-analogue of RebA-G1, called rebaudioside D2 [Glc(β1 → 6)**Glc1**], was obtained as a minor product in the bioconversion reaction of RebA into rebaudioside D [Glc(β1 → 2) **Glc1**] using UDP-Glc as glucosyl donor and the β-glucosyltransferase UGTSL2 enzyme as biocatalyst [41]. Furthermore, a Glc(α1 → 6) extension of **Glc1** of stevioside was demonstrated in a transglucosylation reaction with maltose as donor substrate in the presence of Biozyme L [20].

2.4. Structural analysis of HPLC fraction *F3*

Methylation analysis of HPLC fraction **F3** (RebA+2Glc) showed terminal Glc*p* and 2,3-di-O-substituted Glc*p* (molar ratio ~3:1), and no other multi-O-substituted Glc residues, indicating that no further branching had occurred (Table 3). The presence of 3-, 4- and 6-mono-O-substituted Glc*p* (ratio 11:3:19) indicated elongation of terminal Glc residues, and suggested the occurrence of a mixture of compounds, which was supported by the 1D ^{1}H NMR spectrum of **F3** (Fig. 5). Alkaline treatment of **F3** yielded only RebB (**F1-4S**; Supplementary Information Fig. S7), demonstrating that extensions had only occurred at the steviol C-19 site.

Fraction **F3** was subfractionated by high-pH anion-exchange chromatography (HPAEC) on CarboPac PA-1, yielding two fractions **F3**P1 and **F3**P2 (peak area ratio 3:7), which were isolated for further analysis. MALDI-TOF-MS revealed identical spectra for **F3**P1 and **F3**P2 ($[M+Na]^+$, *m/z* 1312.7; $[M+K]^+$, *m/z* 1329.5), reflecting in both cases the attachment of two Glc residues at RebA (in view of the foregoing at the steviol C-19 site). Methylation analysis of both fractions showed a significant difference between **F3**P1 and **F3**P2 for the amounts of 3-, 4- and 6-mono-O-substituted Glc*p* derivatives (Table 3). Furthermore, the ^{1}H NMR spectra of **F3**P1 and **F3**P2 are clearly different (Fig. 7; enlarged anomeric regions in Supplementary Information Fig. S8).

TOCSY, HSQC and ROESY measurements carried out on HPAEC fraction **F3**P1 afforded the assignment of the ^{1}H/^{13}C resonances stemming from the steviol aglycone (Table 1) and the carbohydrate moieties (Table 2). The ^{1}H and ^{13}C data of the steviol core correspond with those found for RebA (**F1**) and RebA-G1 (**F2**). The same holds for the ^{1}H and ^{13}C signals of the trisaccharide moiety at the steviol C-13 site, indicating that no modifications had occurred at this site, in agreement with the alkaline-treatment results of **F3**. The β-anomeric signals of this moiety are found at $\delta_{H\text{-}1}$ 4.720/$\delta_{C\text{-}1}$ 97.6 (**Glc2**), $\delta_{H\text{-}1}$ 4.810/$\delta_{C\text{-}1}$ 103.5 (**Glc3**) and $\delta_{H\text{-}1}$ 4.700/$\delta_{C\text{-}1}$ 103.8 (**Glc4**). The remaining carbohydrate signals in the ^{1}H and ^{13}C anomeric regions represent the β-anomeric signals of **Glc1** (steviol C-19 site) at $\delta_{H\text{-}1}$ 5.426/$\delta_{C\text{-}1}$ 95.7 and the overlapping α-anomeric signals of **Glc5** and **Glc6′** at $\delta_{H\text{-}1}$ ~4.88/$\delta_{C\text{-}1}$ 99.5 (H-1's also overlap with one of the steviol C-17 protons, δ_H 4.875). The downfield chemical shift value of **Glc1** C-6 (δ_C 67.5; RebA **Glc1** C-6: δ_C 62.2) is

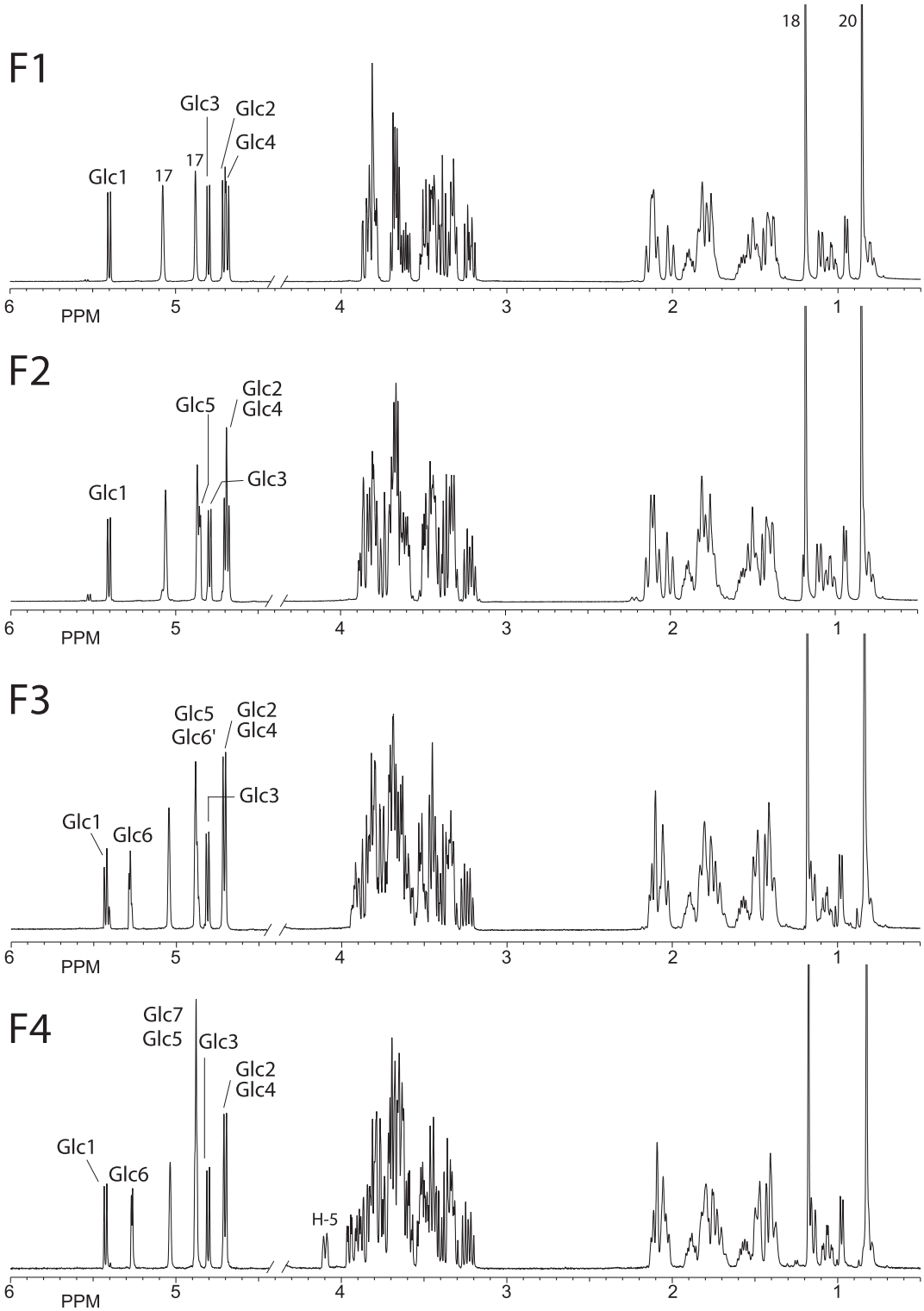

Fig. 5. 500-MHz ^{1}H NMR spectra of HPLC fractions **F1**, **F2**, **F3** and **F4**, recorded in D_2O at 334 K. Enlarged anomeric regions are presented in Supplementary Information Fig. S6. Steviol core C-17, C-18 and C-20 protons are indicated in the spectrum of **F1**. For structures, see Fig. 4.

in accordance with the presence of a → 6)**Glc1**(β1 → C-19 residue. As **Glc5** C-6 showed the same downfield chemical shift as **Glc1** C-6 (δ_C 67.5) and **Glc6**′ had similar ^{13}C values as terminal **Glc5**(α1 → 6) in **F2** (Table 2), the monosaccharide sequence of the carbohydrate moiety at C-19 of **F3**P1 should be **Glc6**′(α1 → 6)**Glc5**(α1 → 6) **Glc1**(β1 → (RebA-G2a) (Fig. 4). The latter sequence is further supported by the inter-residual ROESY cross-peaks between **Glc6**′ H-1 (δ_H 4.875) and **Glc5** H-6a/b (δ_H 3.88/3.65) and between **Glc5** H-1 (δ_H 4.875) and **Glc1** H-6a/b (δ_H 3.89/3.70). Also the methylation analysis data of **F3**P1 (Table 3) are in accordance with this structure. Note that **Glc5** and **Glc6**′ H-1 of the steviol core ester-bound β-isomaltotriose in **F3**P1 ($\delta_{H\text{-}1}$ ~4.88, T = 334 K) resonates clearly

Table 3
Methylation analysis of the carbohydrate moieties in RebA and α-glucosylated RebA products (fractions **F1**-**F5** and **F9**).

Alditol acetate	R_t[a]	Structural feature	Peak area (%)[b]							
			F1	**F2**	**F3**	**F3**P1	**F3**P2	**F4**	**F5**	**F9**
			RebA	+1Glc	+2Glc	+2Glc	+2Glc	+3Glc	+4Glc	+8Glc
2,3,4,6-Hex[c]	1.00	Glc*p*(1→	74	61	50	50	49	45	38	26
2,4,6-Hex	1.16	→3)Glc*p*(1→	–	–	11	–	15	11	23	32
3,4,6-Hex	1.18	→4)Glc*p*(1→	–	–	3	tr[d]	5	tr	tr	tr
2,3,4-Hex	1.22	→6)Glc*p*(1→	–	19	19	33	16	29	24	30
4,6-Hex	1.32	→2,3)Glc*p*(1→	26	20	17	17	15	15	12	8
2,4-Hex	1.39	→3,6)Glc*p*(1→	–	–	–	–	–	tr	3	4

[a] R_t, retention time relative to 1,5-di-*O*-acetyl-2,3,4,6-tetra-*O*-methylglucitol (1.00) on GLC (see Section 4.5).
[b] Averaged rounded-off values from methylation analyses carried out on fractions, isolated from three different incubations with Gtf180-ΔN.
[c] 2,3,4,6-Hex = 1,5-di-*O*-acetyl-2,3,4,6-tetra-*O*-methylhexitol-1-*d*, etc.
[d] tr = trace (<3%).

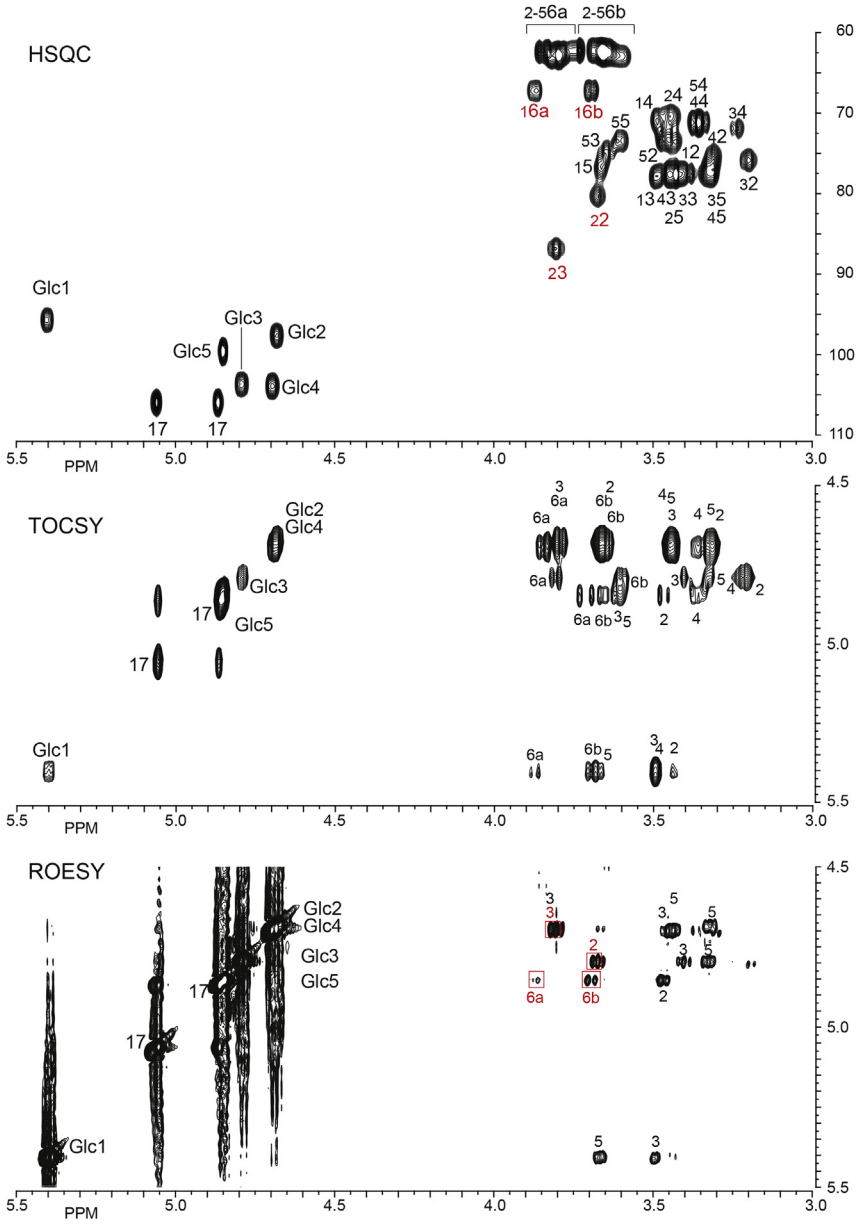

Fig. 6. HSQC, TOCSY (mixing time 200 ms) and ROESY spectra of the carbohydrate part of HPLC fraction **F2** (RebA-G1), recorded in D_2O at 334 K. In the HSQC spectrum, 23 means cross-peak H-3/C-3 of residue **Glc2**, etc.; assignments in red reflect the substituted positions of the residues. In the ROESY spectrum, the inter-residual cross-peaks confirming the **Glc4**(β1 → 3)**Glc2**, **Glc3**(β1 → 2)**Glc2** and **Glc5**(α1 → 6)**Glc1** linkages are indicated with red boxes. (For interpretation of the references to colour in this figure legend, the reader is referred to the web version of this article.)

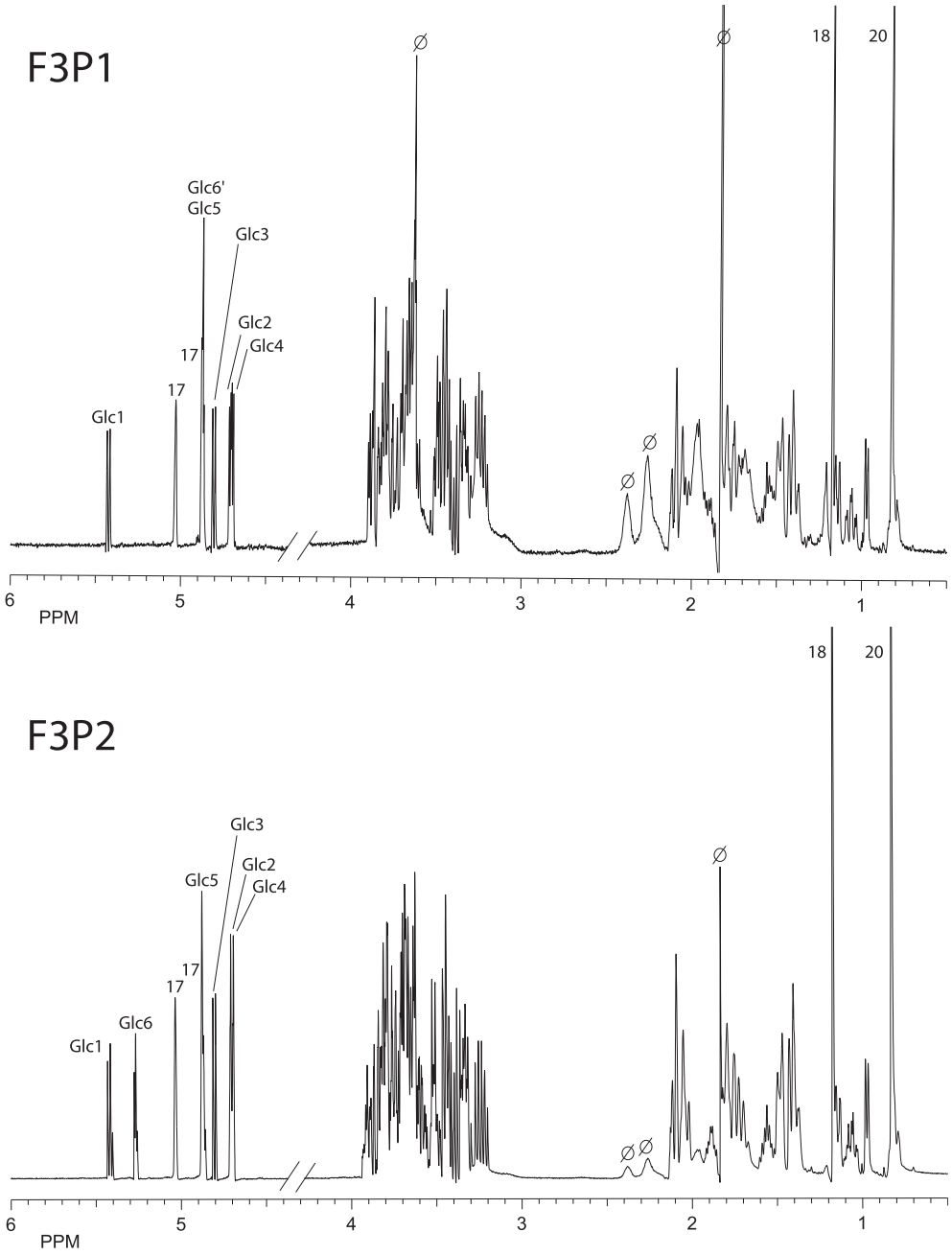

Fig. 7. 500-MHz ^{1}H NMR spectra of HPAEC fractions **F3**P1 and **F3**P2, recorded in D_2O at 334 K. ø means contamination. Enlarged anomeric regions are presented in Supplementary Information Fig. S8. For structures, see Fig. 4.

upfield from the anomeric protons of the terminal and internal Glc(α1 → 6) residues in free β-isomaltotriose (δ_{H-1} ~4.96; T = 300 K) [40]. Furthermore, their H-5 chemical shifts can be used to discriminate between a terminal Glc(α1 → 6) and an internal → 6)Glc(α1 → 6) position: **Glc6′** H-5, δ_H 3.64; **Glc5** H-5, δ_H 3.80.

In a similar way as described for **F3**P1, TOCSY, HSQC and ROESY measurements carried out on HPAEC fraction **F3**P2 afforded the assignment of the ^{1}H/^{13}C resonances stemming from the steviol aglycone (Table 1) and the carbohydrate moieties (Table 2). The steviol core NMR data of **F3**P2 are similar to those of **F3**P1. The same holds for the ^{1}H and ^{13}C signals of the carbohydrate moiety at the steviol C-13 site (for the anomeric regions: **Glc2**, δ_{H-1} 4.715, δ_{C-1} 97.6; **Glc3**, δ_{H-1} 4.810, δ_{C-1} 103.6; **Glc4**, δ_{H-1} 4.702; δ_{C-1} 103.9). These results, together with the alkaline-treatment data of **F3**, indicated that also in **F3**P2 the carbohydrate moiety at the steviol C-13 site was not modified. The remaining carbohydrate signals in the anomeric region of the ^{1}H NMR spectrum of **F3**P2 (Fig. 7; enlarged anomeric region in Supplementary Information Fig. S8) represent a heterogeneous β-anomeric signal of **Glc1** (steviol C-19 site) at δ_H ~5.42, a heterogeneous α-anomeric signal at δ_H ~4.88 (**Glc5**), overlapping with one of the C-17 steviol protons, and a heterogeneous α-anomeric signal at δ_H ~5.28 (**Glc6**). The **Glc1** H-1 signal is clearly built up from two doublets at δ_H 5.425 and 5.410 ($J_{1,2}$ 8.3 Hz; peak ratio 2.7:1.0), the **Glc5** H-1 signal from two doublets at δ_H 4.873 and 4.857 ($J_{1,2}$ 4.1 Hz; peak ratio 2.8:1.0), and the **Glc6** H-1 signal from two doublets at δ_H 5.275 and 5.265 ($J_{1,2}$ 4.3 Hz; peak ratio 2.8:1.0), suggesting the presence of two compounds in

fraction **F3**P2. As H-1 signals of terminal Glc(α1 → 3) and terminal Glc(α1 → 4) residues, when present in a major/minor mixture, are difficult to distinguish by their chemical shifts {compare nigerotriose and maltotriose (300 K) [40]}, the δ_H values of **Glc6** H-1 at 5.275 and 5.265 ppm could reflect the presence of both possibilities.

Inspection of the NMR data of **F3**P2, obtained from combined TOCSY and HSQC experiments (Fig. 8, HSQC spectrum plotted at a high level), showed a downfield **Glc1** C-6 signal at δ_C 67.0, in agreement with a 6-substituted **Glc1** residue, and a downfield **Glc5** C-3 signal at δ_C 81.5, in agreement with a 3-substituted **Glc5** residue [compare with β-isomaltose (α-D-Glc*p*′-(1 → 6)-β-D-Glc*p*: C-6′, δ_C 61.4; C-6, δ_C 66.7) and α-nigerose (α-D-Glc*p*′-(1 → 3)-α-D-Glc*p*: C-3′, δ_C 73.7; C-3, δ_C 80.6)] [42]. ROESY experiments showed inter-residual cross-peaks between **Glc6** H-1 (δ_H 5.27) and **Glc5** H-3 (δ_H 3.79) and between **Glc5** H-1 (δ_H 4.87) and **Glc1** H-6a/b (δ_H 3.91/3.69). Intra-residual H-1–H-2 cross-peaks for **Glc5** and **Glc6** confirmed their α-configurations. Based on these experiments, it was concluded that the major component (~74%) in fraction **F3**P2 contained the **Glc6**(α1 → 3)**Glc5**(α1 → 6)**Glc1**(β1 → glycan at the steviol C-19 site (RebA-G2b) (Fig. 4). Taking into account the methylation analysis of **F3**P2 (Table 3), showing ~75% 3-O-mono-substituted Glc*p* and ~25% 4-O-mono-substituted Glc*p*, it is suggested that the minor glycan at the steviol C-19 site is **Glc6**(α1 → 4)**Glc5**(α1 → 6)**Glc1**(β1 → (RebA-G2c) (Fig. 4). In summary, the three components present in fraction **F3** occur in a molar ratio RebA-G2a:RebA-G2b:RebA-G2c of about 40:47:13. Note that anomeric chemical shift differences exist between terminal Glc(α1 → 3)/Glc(α1 → 4) residues in free oligosaccharides [terminal Glc(α1 → 3): δ_{H-1} ~5.36; terminal Glc(α1 → 4): δ_{H-1} ~5.40; T = 300 K] [40] and steviol core ester-bound trisaccharides [**Glc6**(α1 → 3), δ_{H-1} ~5.275; **Glc6**(α1 → 4), δ_{H-1} ~5.265; T = 334 K].

2.5. Structural analysis of HPLC fraction *F4*

Methylation analysis of HPLC fraction **F4** (RebA+3Glc) showed the presence of 6- and 3-mono-O-substituted Glc*p* in the molar ratio 2.6:1.0; furthermore, the molar ratio of terminal and 2,3-di-O-substituted Glc*p* is 3:1 (Table 3). Although the integration of the anomeric protons in the ^{1}H NMR spectrum of **F4** (Fig. 5) suggest the presence of one major component, in view of the mentioned structures present in fraction **F3**, it would be expected that also fraction **F4** contains a mixture of different compounds with the same molecular mass. As already discussed for **F2** and **F3**, also in **F4** the extra α-linked Glc residues are only located at the steviol C-19 site [alkaline treatment of **F4** yielded only RebB (**F1-4S**; Supplementary Information Fig. S7)]. The ^{1}H/^{13}C NMR assignments of the **F4** steviol aglycone and carbohydrate moieties, derived from TOCSY, HSQC and ROESY measurements, are presented in Tables 1 and 2, respectively (spectra not shown).

Inspection of the ^{1}H NMR spectrum of **F4** (Fig. 5) revealed the characteristic peak pattern of the steviol core, comprising the two steviol H-17 signals in the carbohydrate anomeric region and further signals in the upfield region 0.80–2.20 ppm (Table 1). In the anomeric region, the three β-anomeric proton resonances stemming from the carbohydrate moiety at the steviol C-13 site [**Glc2**: δ_{H-1} 4.700 (with δ_{C-1} 97.6); **Glc3**: δ_{H-1} 4.802 (with δ_{C-1} 103.6); **Glc4**: δ_{H-1} 4.700 (with δ_{C-1} 103.7)] are detected (Table 2). The **Glc1** H-1–H6b (H-1, δ_H 5.425) and C-1–C-6 (C-6, δ_C 67.0) chemical shift sets correspond with the → 6)Glc(β1 → C-19 residue, just like in **F2** and **F3**. The three α-anomeric signals reflect the glycan extension at **Glc1**. The **Glc7** ^{1}H and ^{13}C sets are in accordance with a terminal Glc(α1 → 6) residue (e.g. H-1, δ_H 4.875, $J_{1,2}$ <4 Hz; C-1, δ_C 99.3; C-3, δ_C 74.5; C-6, δ_C 62.5; compare with the sets of **Glc5** in **F2** and **Glc6** in **F3**P1). The **Glc5** ^{1}H and ^{13}C sets indicate an internal → 3)Glc(α1 → 6) residue (e.g. H-1, δ_H 4.875, $J_{1,2}$ <4 Hz; C-1, δ_C 99.2; C-3, δ_C 82.3; C-6, δ_C 62.5; compare with the sets of **Glc5** in **F3**P2). Finally, the **Glc6** ^{1}H and ^{13}C sets show the presence of an internal → 6)Glc(α1 → 3) residue (e.g. H-1, δ_H 5.259, $J_{1,2}$ <4 Hz with C-1, δ_C 101.2; H-5, δ_H 4.09 with C-5, δ_C 72.2; C-3, δ_C 75.0; C-6, δ_C 67.0). Furthermore, ROESY experiments revealed inter-residual cross-peaks between **Glc7** H-1 (δ_H 4.875) and **Glc6** H-6a/b (δ_H 3.94/3.64), between **Glc6** H-1 (δ_H 5.259) and **Glc5** H-3 (δ_H 3.77) and between **Glc5** H-1 (δ_H 4.875) and **Glc1** H-6a/b (δ_H 3.89/3.70). Taken together, the various results of fraction **F4** indicated the presence of a major product (~73%), having a carbohydrate moiety consisting of **Glc7**(α1 → 6)**Glc6**(α1 → 3)**Glc5**(α1 → 6)**Glc1**(β1 → (RebA-G3a) at the steviol C-19 site, i.e. an elongation of RebA-G2b with a Glc(α1 → 6) residue (Fig. 4). Note that **Glc6** H-1 (δ_H 5.259, 334 K) of the steviol core ester-bound glycan in **F4**, oriented in an internal → 6)Glc(α1 → 3) position, resonates upfield from the anomeric proton of internal → 6)Glc(α1 → 3) residues (δ_H ~5.33, T = 300 K) in similar free oligosaccharides, e.g. Glc(α1 → 6)Glc(α1 → 3)Glc(α1 → 6)Glc [28]. Taking into account composite models of α-D-glucans generated from sucrose using wild-type and mutant Gtf180-ΔN glucansucrases as biocatalyst [28,30,31], the

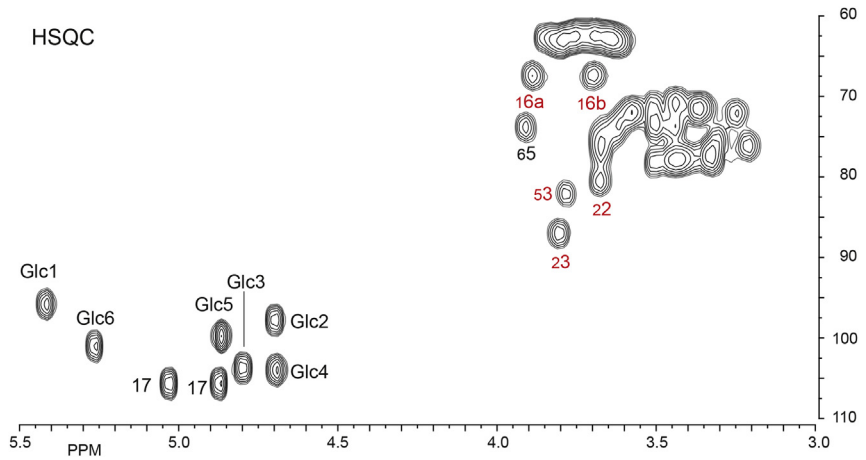

Fig. 8. HSQC spectrum (200 ms) of the carbohydrate part of HPAEC fraction **F3**P2, plotted at high level (resonances from RebA-G2b). 23 means cross-peak H-3/C-3 of residue **Glc2**, etc.; assignments in red reflect the substituted positions of the residues. Note **Glc6** H-5/C-5 (δ 3.93/73.4), stemming from terminal Glc(α1 → 3). (For interpretation of the references to colour in this figure legend, the reader is referred to the web version of this article.)

structure of one of the expected minor products is hypothesized to be an elongation of RebA-G2a with a Glc(α1 → 6) residue [**Glc7**(α1 → 6)**Glc6**(α1 → 6)**Glc5**(α1 → 6)**Glc1**(β1 →].

2.6. Structural analysis of HPLC fractions ***F5-F9***

As is evident from the HPLC profile in Fig. 3, fractions **F5** (RebA+4Glc) to **F9** (RebA+8Glc) represent complex mixtures of RebA derivatives. Inspection of the 1D ^{1}H NMR spectra of **F5** to **F9** (spectra not shown) learned that the steviol core regions (0.80–2.20 ppm) are identical and the carbohydrate bulk regions (3.20–4.20 ppm) similar to those in the 1D ^{1}H NMR spectra of **F3** and **F4**. When treated with alkali, each fraction was converted into RebB (**F1-4S**; Supplementary Information Fig. S7), meaning that also in the case of **F5** to **F9** α-glucosylation had only occurred at the steviol C-19 glucosyl moiety of RebA. The patterns of anomeric signals in the ^{1}H NMR spectra of **F5** to **F9** are comparable with those of **F3** and **F4**, indicating that the elongated carbohydrate chains at the steviol C-19 site of **F5** to **F9** are built up from (α1 → 6)- and (α1 → 3)-linked Glc residues. More specifically, the spectra showed relative increase in intensities of the H-1 resonance at δ_H 5.25 and the H-5 resonance at δ_H 4.10, derived from internal → 6) Glc(α1 → 3) residues, and the H-1 resonance at δ_H 4.87, derived from terminal Glc(α1 → 6) and internal → 6)Glc(α1 → 6) residues. Methylation analysis of these high-molecular-mass fractions showed an increase of (α1 → 6) and (α1 → 3) linkages towards almost equal molar amounts (Table 3; only traces of 4-linked Glc*p* were observed), suggesting the preference of the wild-type Gtf180-ΔN enzyme for the synthesis of alternating (α1 → 6)/(α1 → 3) linkages in the major formed RebA derivatives. Furthermore, the finding of low amounts of 3,6-di-O-substituted Glc*p* residues in the methylation analysis of these fractions reflects also the possibilities of branching.

3. Conclusions

Over the years, several types of carbohydrate-active enzymes have been used in the glycosylation reactions of steviol glycosides (see review Ref. [3]). With respect to trans-α-glucosylations, cyclodextrin glycosyltransferase systems, introducing elongations with α-D-Glc*p*-(1 → 4) units at both the steviol C-13 and C-19 sites of stevioside, rubusoside and rebaudioside A (RebA), gained great attention. In these bioconversions, glucose donors such as cyclodextrins, maltodextrins and starches are used. But also other α-glucosidase transglycosylation systems were investigated, i.e. glucansucrase enzymes combined with sucrose as glucose donor.

Using alternansucrase from *Leuconostoc citreum* SK24.002 as biocatalyst, stevioside (Fig. 1) could be converted into a mixture of nine products, including three mono-, three di- and three tri-α-glucosylated stevioside derivatives. Two products were characterized in detail, showing elongations of the terminal Glc(β1 → 2) residue of the β-sophorosyl disaccharide at the steviol C-13 site with a Glc(α1 → 6) unit and with a Glc(α1 → 3)Glc(α1 → 6) Glc(α1 → 3) trisaccharide [43–45]. When incubated with sucrose alone, alternansucrase produces a glucan with alternating (α1 → 3) and (α1 → 6) linkages, called alternan [46].

Recent studies in our research group have shown that (mutant) Gtf180-ΔN glucansucrase of *Lb. reuteri* strain 180 introduces glucose residues from sucrose into RebA, specifically at the C-19 site. In this report the structural analysis of the formed products with wild-type Gtf180-ΔN glucansucrase as biocatalyst has been described in detail. Structural biological aspects, including comparison of transglycosylation activities and differences in conversion percentages of wild-type and 82 mutant Gtf180-ΔN glucansucrase enzymes, molecular docking studies of the Gtf180-ΔN – RebA complex, and sweetness/bitterness tests will be described elsewhere [te Poele et al., manuscript in preparation]. As a first step, the Glc(β1 → C-19 residue of RebA was found to be elongated with a Glc(α1 → 6) residue (RebA-G1). Further extensions, up to eight Glc units, comprised mainly Glc(α1 → 6) and Glc(α1 → 3) residues; in the trisaccharide, elongation evidence for a termination with a Glc(α1 → 4) residue was found. The major higher α-glucosylated RebA products are built up by elongation of the Glc(α1 → 6)Glc(β1 → C-19 moiety with alternating (α1 → 3)/(α1 → 6)-linked Glc units, accompanied by products with only (α1 → 6)-linked sequences in lesser amounts. In the higher-molecular-mass components also 3,6-branching is indicated.

4. Experimental

4.1. Steviol glycoside substrates and glucansucrase enzyme

Rebaudioside A (RebA) was purchased from Sigma-Aldrich Chemie (Zwijndrecht, The Netherlands) and stevioside (Ste) from Wako Pure Chemical Industries (Osaka, Japan). Rebaudioside B (RebB) was prepared by alkaline treatment of RebA (see Section 4.3). The *Lactobacillus reuteri* 180 glucansucrase enzyme Gtf180-ΔN [117-kDa N-terminally truncated (741 residues) fragment of the wild-type Gtf180 full-length protein] was produced and purified as described [47,48].

4.2. Preparation of α-D-glucosylated rebaudioside A products

Incubations of RebA (50 mM) were performed in 5 mL 25 mM sodium acetate (pH 4.7), containing 1 mM $CaCl_2$, in the presence of 10 U/mL Gtf180-ΔN enzyme at 37 °C and 24 h. Two batches of 1.0 M sucrose donor substrate were added at t = 0 and t = 3 h, respectively. One unit (U) of enzyme is defined as the amount of enzyme required for producing 1 μmol fructose from sucrose per min in reaction buffer, containing 1.0 M sucrose at 37 °C. In this case, 1 U corresponded to 0.038 mg Gtf180-ΔN. The full rationale for these incubation conditions will be described in detail elsewhere [te Poele et al., manuscript in preparation]. The pool of glucosylated RebA products was isolated by solid-phase extraction (SPE) using a Strata-X 33μ Polymeric Reversed Phase column (Phenomenex, Utrecht, The Netherlands). Briefly, the SPE column was conditioned with 6 bed volumes methanol and subsequently equilibrated with 6 bed volumes de-ionized water. After loading of the sample, the column was washed with 6 bed volumes de-ionized water to remove enzyme, glucose, fructose, gluco-oligo/polysaccharides and residual sucrose. Then, the mixture of RebA products was eluted with 6 bed volumes 50% acetonitrile. Subsequently, the mixture was fractionated on a Luna 10 μm NH_2 semi-preparative chromatography column (250 mm × 10 mm, Phenomenex), using an UltiMate 3000 HPLC system (ThermoFisher Scientific, Amsterdam, The Netherlands), equipped with a VWD-3000 UV-VIS detector (monitoring at 210 nm). Separations were obtained at a flow-rate of 4.6 mL/min under gradient elution conditions (solvent A = acetonitrile; solvent B = 0.025% aqueous acetic acid), starting with a 2-min isocratic step with 80% solvent A in B followed by a linear gradient of 80 to 50% solvent A in B over 38 min. The manually collected fractions were evaporated to dryness under a stream of nitrogen, and the residues were re-dissolved in de-ionized water and directly lyophilized. Fresh newly dissolved samples were used for analysis.

4.3. Alkaline hydrolysis

To release the carbohydrate moiety linked to the C-19 carboxyl group, 4 mg RebA and 4 mg of each transglucosylated product were

individually dissolved in 1 mL 1.0 M NaOH and the solutions were heated at 80 °C for 2.5 h, then cooled down, and neutralized with 6 M HCl. The modified product fractions were isolated using Strata-X 33μ Polymeric Reversed Phase columns (Phenomenex), as described in Section 4.2.

4.4. High-pH anion-exchange chromatography

High-pH anion-exchange chromatography (HPAEC) was performed on a Dionex DX500 workstation (Dionex, Amsterdam, The Netherlands), equipped with a CarboPac PA-1 column (250 × 9 mm; Dionex) and an ED40 pulsed amperometric detector, using a linear gradient from 30 mM to 265.2 mM sodium acetate in 100 mM NaOH (3 mL/min) over 26 min. Collected fractions were immediately neutralized with 4 M acetic acid, desalted on Strata-X 33μ Polymeric Reversed Phase columns (Phenomenex), using 50% aqueous acetonitrile as eluent, and lyophilized.

4.5. Methylation analysis

Steviol glycoside samples were permethylated using CH_3I and solid NaOH in $(CH_3)_2SO$, as described previously [49], then hydrolyzed with 2 M trifluoroacetic acid (2 h, 120 °C) to give the mixture of partially methylated monosaccharides. After evaporation to dryness, the mixture, dissolved in H_2O, was reduced with $NaBD_4$ (2 h, room temperature). Subsequently, the solution was neutralized with 4 M acetic acid and boric acid was removed by repeated co-evaporation with methanol. The obtained partially methylated alditol samples were acetylated with 1:1 acetic anhydride-pyridine (30 min, 120 °C). After evaporation to dryness, the mixtures of partially methylated alditol acetates, dissolved in dichloromethane, were analyzed by GLC-EI-MS on an EC-1 column (30 m × 0.25 mm; Alltech), using a GCMS-QP2010 Plus instrument (Shimadzu Kratos Inc., Manchester, UK) and a temperature gradient (140–250 °C at 8 °C/min) [50].

4.6. Mass spectrometry

Matrix-assisted laser desorption ionization time-of-flight mass spectrometry (MALDI-TOF-MS) was performed on an Axima™ mass spectrometer (Shimadzu Kratos Inc.), equipped with a nitrogen laser (337 nm, 3 ns pulse width). Positive-ion mode spectra were recorded using the reflector mode at a resolution of 5000 FWHM and delayed extraction (450 ns). Accelerating voltage was 19 kV with a grid voltage of 75.2%. The mirror voltage ratio was 1.12 and the acquisition mass range was 200–6000 Da. Samples were prepared by mixing on the target 1-μL sample solutions with 1 μL aqueous 10% 2,5-dihydroxybenzoic acid in 70% acetonitrile as matrix solution.

4.7. NMR spectroscopy

Resolution-enhanced 1D/2D 500-MHz $^1H/^{13}C$ NMR spectra were recorded in D_2O on a Bruker DRX-500 spectrometer (Bijvoet Center, Department of NMR Spectroscopy, Utrecht University). To avoid overlap of anomeric signals with the HOD signal, the spectra were run at 334 K. Data acquisition was done with Bruker Topspin 2.1. Before analysis, samples were exchanged twice in D_2O (99.9 atom% D, Cambridge Isotope Laboratories, Inc., Andover, MA) with intermediate lyophilization, and then dissolved in 0.6 mL D_2O. It should be noted that during longer stay in aqueous solution, partial degradation of steviol glycosides can occur due to loss of the carbohydrate moiety from the steviol C-19 carboxyl group and possible formation of the Δ^{15-16} isomer and the Δ^{16-17} hydration products [51,52]. Therefore, fresh solutions of ~4 mg/mL (~4 mM) were used for all NMR measurements. Suppression of the HOD signal was achieved by applying a WEFT (water eliminated Fourier transform) pulse sequence for 1D NMR experiments and by a presaturation of 1 s during the relaxation delay in 2D experiments. The 2D TOCSY spectra were recorded using an MLEV-17 (composite pulse devised by Levitt et al.) [53] mixing sequence with spin-lock times of 20, 50, 100 and 200 ms. The 2D ^1H-^1H ROESY spectra were recorded using standard Bruker XWINNMR software with a mixing time of 200 ms. The carrier frequency was set at the downfield edge of the spectrum in order to minimize TOCSY transfer during spin-locking. Natural abundance 2D ^{13}C-^1H HSQC experiments (^1H frequency 500.0821 MHz, ^{13}C frequency 125.7552 MHz) were recorded without decoupling during acquisition of the ^1H FID. The NMR data were processed using the MestReNova 9 program (Mestrelab Research SL, Santiago de Compostella, Spain). Chemical shifts (δ) are expressed in ppm by reference to internal acetone (δ_H 2.225 for ^1H and δ_C 31.07 for ^{13}C).

Acknowledgements

This work was financially supported by EU project NOVOSIDES FP7-KBBE-2010-4-265854 (LD).

Appendix. Supplementary information

Supplementary data related to this article can be found at http://dx.doi.org/10.1016/j.carres.2017.01.008.

References

[1] J.E. Brandle, A.N. Starratt, M. Gijzen, Can. J. Plant Sci. 78 (1998) 527–536.
[2] S. Ceunen, J.M.C. Geuns, J. Nat. Prod. 76 (2013) 1201–1228.
[3] G.J. Gerwig, E.M. te Poele, L. Dijkhuizen, J.P. Kamerling, Adv. Carbohydr. Chem. Biochem. 73 (2016) 1–72.
[4] J.M.C. Geuns, Phytochemistry 64 (2003) 913–921.
[5] S.K. Goyal, Samsher, R.K. Goyal, Int. J. Food Sci. Nutr. 61 (2010) 1–10.
[6] S. Madan, S. Ahmad, G.N. Singh, K. Kohli, Y. Kumar, R. Singh, M. Garg, Indian J. Nat. Prod. Resour. 1 (2010) 267–286.
[7] M. Puri, D. Sharma, A.K. Tiwari, Biotechnol. Adv. 29 (2011) 781–791.
[8] E. Gupta, S. Purwar, S. Sundaram, G.K. Rai, J. Med. Plants Res. 7 (2013) 3343–3353.
[9] R.S. McQuate, Food Technol. 65 (2011) 1–13.
[10] European food safety authority, EFSA J. 8 (1537) (2010) 1–84.
[11] EU Commission, Commission regulation (EU) No. 1131/2011, Off. J. Eur. Union L295 (2011) 205–211.
[12] G. Brahmachari, L.C. Mandal, R. Roy, S. Mondal, A.K. Brahmachari, Arch. Pharm. Chem. Life Sci. 1 (2011) 5–19.
[13] R. Lemus-Mondaca, A. Vega-Gálvez, L. Zura-Bravo, K. Ah-Hen, Food Chem. 132 (2012) 1121–1132.
[14] S.K. Yadav, P. Guleria, Crit. Rev. Food Sci. Nutr. 52 (2012) 988–998.
[15] N. Shivanna, M. Naika, F. Khanum, V.K. Kaul, J. Diabetes Complicat. 27 (2013) 103–113.
[16] M. Darise, K. Mizutani, R. Kasai, O. Tanaka, S. Kitahata, S. Okada, S. Ogawa, F. Murakami, F.-H. Chen, Agric. Biol. Chem. 48 (1984) 2483–2488.
[17] U. Mani, G. Dubois, I. Prakash, Molecules 17 (2012) 4186–4196.
[18] G.E. DuBois, R.A. Stephenson, J. Med. Chem. 28 (1985) 93–98.
[19] Y. Fukunaga, T. Miyata, N. Nakayasu, K. Mizutani, R. Kasai, O. Tanaka, Agric. Biol. Chem. 53 (1989) 1603–1607.
[20] S.V. Lobov, R. Kasai, K. Ohtani, O. Tanaka, K. Yamasaki, Agric. Biol. Chem. 55 (1991) 2959–2965.
[21] K. Ohtani, Y. Aikawa, Y. Fujisawa, R. Kasai, O. Tanaka, K. Yamasaki, Chem. Pharm. Bull. 39 (1991) 3172–3174.
[22] K. Ohtani, Y. Aikawa, H. Ishikawa, R. Kasai, S. Kitahata, K. Mizutani, S. Doi, M. Nakaura, O. Tanaka, Agric. Biol. Chem. 55 (1991) 449–453.
[23] O. Tanaka, Pure Appl. Chem. 69 (1997) 675–683.
[24] F. Ye, R. Yang, X. Hua, Q. Shen, W. Zhao, W. Zhang, LWT – Food Sci. Technol. 51 (2013) 524–530.
[25] I. Prakash, A. Markosyan, C. Bunders, Foods 3 (2014) 162–175.
[26] H. Leemhuis, T. Pijning, J.M. Dobruchowska, S.S. van Leeuwen, S. Kralj, B.W. Dijkstra, L. Dijkhuizen, J. Biotechnol. 163 (2013) 250–272.
[27] T. Desmet, W. Soetaert, P. Bojarová, V. Kren, L. Dijkhuizen, V. Eastwick-Field, A. Schiller, Chem. Eur. J. 18 (2012) 10786–10801.
[28] S.S. van Leeuwen, S. Kralj, I.H. van Geel-Schutten, G.J. Gerwig, L. Dijkhuizen, J.P. Kamerling, Carbohydr. Res. 343 (2008) 1237–1250.
[29] X. Meng, J.M. Dobruchowska, T. Pijning, G.J. Gerwig, L. Dijkhuizen, J. Agric.

Food Chem. 64 (2016) 433–442.
[30] S.S. van Leeuwen, S. Kralj, G.J. Gerwig, L. Dijkhuizen, J.P. Kamerling, Biomacromolecules 9 (2008) 2251–2258.
[31] S.S. van Leeuwen, S. Kralj, W. Eeuwema, G.J. Gerwig, L. Dijkhuizen, J.P. Kamerling, Biomacromolecules 10 (2009) 580–588.
[32] K. Yamasaki, H. Kohda, T. Kobayashi, R. Kasai, O. Tanaka, Tetrahedron Lett. 13 (1976) 1005–1008.
[33] H. Kohda, R. Kasai, K. Yamasaki, K. Murakami, O. Tanaka, Phytochemistry 15 (1976) 981–983.
[34] A.S. Dacome, C.C. da Silva, C.E.M. da Costa, J.D. Fontana, J. Adelmann, S.C. da Costa, Process Biochem. 40 (2005) 3587–3594.
[35] W.E. Steinmetz, A. Lin, Carbohydr. Res. 344 (2009) 2533–2538.
[36] M. Ohta, S. Sasa, A. Inoue, T. Tamai, I. Fujita, K. Morita, F. Matsuura, J. Appl. Glycosci. 57 (2010) 199–209.
[37] V. Pieri, A. Belancic, S. Morales, H. Stuppner, J. Agric. Food Chem. 59 (2011) 4378–4384.
[38] V.S.P. Chaturvedula, I. Prakash, Eur. J. Med. Plants 2 (2012) 57–65.
[39] J.G. Napolitano, C. Simmler, J.B. McAlpine, D.C. Lankin, S.-N. Chen, G.F. Pauli, J. Nat. Prod. 78 (2015) 658–665.
[40] S.S. van Leeuwen, B.R. Leeflang, G.J. Gerwig, J.P. Kamerling, Carbohydr. Res. 343 (2008) 1114–1119.
[41] I. Prakash, C. Bunders, K.P. Devkota, R.D. Charan, C. Ramirez, M. Parikh, A. Markosyan, Nat. Prod. Commun. 9 (2014) 1135–1138.
[42] S.S. van Leeuwen, Thesis Utrecht University, The Netherlands, 2007, pp. 31–55.
[43] A. Musa, M. Miao, T. Zhang, B. Jiang, Food Chem. 146 (2014) 23–29.
[44] A. Musa, M.A.A. Gasmalla, M. Miao, T. Zhang, W. Aboshora, A. Eibaid, B. Jiang, J. Acad. Indus. Res. 2 (2014) 593–598.
[45] A. Musa, M. Miao, M.A.A. Gasmalla, T. Zhang, A. Eibaid, W. Aboshora, B. Jiang, J. Mol. Catal. B Enzym. 116 (2015) 106–112.
[46] G.L. Côté, J.F. Robyt, Carbohydr. Res. 101 (1982) 57–74.
[47] S. Kralj, G.H. van Geel-Schutten, M.J.E.C. van der Maarel, L. Dijkhuizen, Microbiology 150 (2004) 2099–2112.
[48] X. Meng, J.M. Dobruchowska, T. Pijning, C.A. López, J.P. Kamerling, L. Dijkhuizen, J. Biol. Chem. 289 (2014) 32773–32782.
[49] I. Ciucanu, F. Kerek, Carbohydr. Res. 131 (1984) 209–217.
[50] J.P. Kamerling, G.J. Gerwig, in: J.P. Kamerling, G.-J. Boons, Y.C. Lee, A. Suzuki, N. Taniguchi, A.G.J. Voragen (Eds.), Comprehensive Glycoscience – From Chemistry to Systems Biology, vol. 2, Elsevier Ltd, Oxford, 2007, pp. 1–68.
[51] I. Prakash, G.E. DuBois, J.F. Clos, K.L. Wilkens, L.E. Fosdick, Food Chem. Toxicol. 46 (2008) S75–S82.
[52] I. Prakash, J.F. Clos, V.S.P. Chaturvedula, Food Res. Int. 48 (2012) 65–75.
[53] M.H. Levitt, R. Freeman, T. Frenkiel, J. Magn. Reson 47 (1982) 328–330.